

The phase of the radio and X-ray pulses of PSR B1937+21

G. Cusumano¹, W. Hermsen², M. Kramer³, L. Kuiper², O. Löhmer⁴, E. Massaro⁵, T. Mineo¹, L. Nicastro¹, and B.W. Stappers⁶

¹ Istituto di Astrofisica Spaziale e Fisica Cosmica - Sezione di Palermo, CNR, Via Ugo La Malfa 153, I-90146, Palermo, Italy

² SRON National Institute for Space Research, Sorbonnelaan 2, 3584 CA Utrecht, The Netherlands

³ University of Manchester, Jodrell Bank Observatory, Macclesfield, Cheshire SK11 9DL, UK

⁴ Max-Planck-Institut für Radioastronomie, Auf dem Hügel 69, D-53121 Bonn, Germany

⁵ Dipartimento di Fisica, Università La Sapienza, Piazzale A. Moro 2, I-00185, Roma, Italy; Istituto di Astrofisica Spaziale e Fisica Cosmica - Sezione di Roma, CNR, Via del Fosso del Cavaliere, I-00100 Roma, Italy

⁶ ASTRON, Postbus 2, 7990 AA Dwingeloo, The Netherlands; Astronomical Institute "Anton Pannekoek", University of Amsterdam, Kruislaan 403, 1098 SJ Amsterdam, The Netherlands

Received:; accepted:.

Abstract. We present timing and spectral results of PSR B1937+21, the fastest known millisecond pulsar ($P \simeq 1.56$ ms), observed with RXTE. The pulse profile, detected up to ~ 20 keV, shows a double peak with the main component much stronger than the other. The peak phase separation is 0.526 ± 0.002 and the pulsed spectrum over the energy range 2–25 keV is well described by a power law with a photon index equal to 1.14 ± 0.07 . We find that the X-ray pulses are closely aligned in phase with the giant pulses observed in the radio band. This results suggest that giant radio pulses and X-ray pulses originate in the same region of the magnetosphere due to a high and fluctuating electron density that occasionally emits coherently in the radio band. The X-ray events, however, do not show any clustering in time indicating that no X-ray flares are produced.

Key words. Stars: neutron – pulsars: individual: PSR B1937+21 – X-rays: stars

1. Introduction

Millisecond radio pulsars (MSPs) differ from ordinary pulsars for their short spin period in the range 1.5–30 ms and for their low spin-down rate of $\dot{P} < 10^{-19}$ s s⁻¹. They are presumably very old objects, with spin down ages of $\tau \sim 10^9$ – 10^{10} yr and low surface magnetic fields $B \simeq 10^8$ – 10^{10} G. MSPs are believed to be recycled by having accreted mass and angular momentum from an evolving companion star (Alpar et al. 1982). About 50% of all X-ray detected rotation-powered pulsars are MSPs and their X-ray emission seems to have characteristics similar to ordinary pulsars with both thermal and non-thermal components. The former can be described by a modified black body generally peaking in the soft X-ray range, while the latter is characterized by a power-law like spectrum over a broad energy band. Data available up to now, however, leave open the debate about the actual presence of thermal emission from MSPs. The spectra of the few MSPs for which thermal models have been claimed, can also be

modeled either with curved or broken power laws (Becker & Aschenbach 2002).

PSR B1937+21 was the first MSP discovered (Backer et al. 1982) and, with the period of 1.56 ms, it remains the most rapidly rotating neutron star presently known. The distance estimated from the observed dispersion measure (DM) and from a model for the Galactic free electron distribution (Taylor & Cordes 1993, Cordes & Lazio 2002) is 3.6 kpc (see also discussion in Nicastro et al. 2003). Its spin down luminosity is $\dot{E} \sim 1.1 \times 10^{36}$ erg s⁻¹ and the dipolar magnetic field component at the star surface is $\sim 4.1 \times 10^8$ G. Like the Crab pulsar (Lundgren et al. 1995), PSR B0540–69 (Johnston & Romani 2003) and the other MSP PSR B1821–24 (Romani & Johnston), PSR B1937+21 exhibits sporadic emission of giant pulses in the radio band (Sallmen & Backer 1995; Cognard et al. 1996, Kinkhabwala et al. 2000). Such pulses are extremely short events ($\tau < 0.3$ μ s at 2.38 GHz) confined to small phase windows trailing the main and interpulse.

X-ray emission from this pulsar was detected by ASCA (Takahashi et al. 2001) above 2 keV, with a pulse profile characterized by a single sharp peak and a pulsed fraction of 44%. Comparing the X-ray and radio phase ar-

rival times, these authors claimed that the X-ray pulse is aligned with the radio interpulse. Later, BeppoSAX detected pulsed emission from PSR B1937+21 (Nicastro et al. 2002, 2003) and the pulse profile was found to show a double peak pattern with a phase separation from P1 to P2 of 0.52 ± 0.02 and a significance of the second peak of $\sim 5\sigma$. The BeppoSAX data did not allow to study the relative alignment between X-ray and radio pulses, because the timing did not maintain the necessary accuracy to UTC.

In this letter we present the results of the timing and spectral analysis of a RXTE observation of PSR B1937+21. We compare the absolute phases of the X-ray and radio pulsed signals and show that the X-ray peaks are phase aligned with the radio giant pulses (Section 3). The pulsed spectrum is derived in Section 4.

2. X-ray and Radio Observations and Data Reduction

The RXTE pointings at PSR B1937+21 were performed between February 22 and February 27, 2002. The total exposure times were about 140,000 s for the PCA units 0, 2 and 3, and about 20,000 s for the units 1 and 4. Standard selection criteria were applied to the observation data excluding time intervals corresponding to South Atlantic Anomaly passages and when the Earth's limb was closer than 10 degrees and the angular distance between the source position and the pointing direction of the satellite was larger than $0^{\circ}02$. We verified that the selection of all PCA detector layers, instead of those from the top layer only, increased significantly the S/N ratio of the pulsation and adopted this choice for our timing analysis. We used only data obtained with the PCA (Jahoda et al. 1996) accumulated in "Good Xenon" telemetry mode for the timing and spectral analysis. Events are time-tagged with a $1\ \mu\text{s}$ accuracy with respect to the spacecraft clock and with an absolute time accuracy of $5\text{--}8\ \mu\text{s}$ with respect to UTC. The UTC arrival times of all selected X-ray events were first converted to the Solar System Barycentre using the (J2000) pulsar position given in Table 1 and the JPL2000 planetary ephemeris (DE200, Standish 1982).

The radio ephemeris of PSR B1937+21 were obtained from high precision timing observations made with the 100-m Effelsberg radiotelescope in Bonn, Germany, and with the Westerbork Synthesis Radio Telescope (WSRT) in Westerbork, The Netherlands. From October 1996 timing data were collected at 1410 MHz with the Effelsberg telescope once per month, with a typical observing time of 3×7 min. Two circular polarized signals were mixed down to an intermediate frequency, detected and coherently de-dispersed in a digital filterbank (Backer et al. 1997). The data were time stamped with clock information from a local hydrogen maser clock and later synchronized to UTC(NIST) using the signals from the Global Positioning System (GPS). Pulse times-of-arrival (TOAs) were calculated from a fit of a synthetic template to the observed profile with a template matching procedure (for details

Table 1. JPL DE200 ephemeris of PSR B1937+21 (data from Effelsberg and WSRT observations).

Parameter	Value
Right Ascension (J2000)	$19^{\text{h}} 39^{\text{m}} 38.560096(6)$
Declination (J2000)	$21^{\circ} 34' 59'' 13552(13)$
Proper motion in R.A. (mas yr^{-1})	$-0.05(2)$
Proper motion in Dec (mas yr^{-1})	$-0.47(4)$
Frequency (Hz)	$641.928244534462(3)$
Frequency derivative (Hz s^{-1})	$-4.331046(13) \times 10^{-14}$
Frequency 2nd derivative (Hz s^{-2})	$8.9(1.8) \times 10^{-27}$
Epoch of the period (MJD)	52328.0
DM ($\text{cm}^{-3} \text{pc}$)	71.02666(16)
DM derivative ($\text{pc cm}^{-3} \text{yr}^{-1}$)	$-2.10(17)$
Epoch validity start/end (MJD)	50360 – 52867
Epoch of arrival time [†] (MJD)	52332.167314839268(11)
Frequency of arrival time (MHz)	1409.300
Post-fit timing rms (ns)	910

Note: Uncertainties quoted are in the last digit(s) and represent 2σ estimates (twice the formal TEMPO errors). The Epoch of arrival time refers to the maximum of the main peak in the integrated radio profile.

[†] at Effelsberg telescope

see Lange et al. 2001). TOA errors for PSR B1937+21 lie in the range 80–200 ns making it one of the most precise objects for pulsar timing.

The WRST observations were performed since July 1999 at center frequencies of 840 and 1380 MHz using the Dutch pulsar machine PuMa (Voûte et al. 2002). The observing and analysis procedure to produce the WSRT TOAs were similar to those at Effelsberg except that linear polarisations were recorded. The dual frequency nature of the WSRT data set allowed us to accurately monitor dispersion measure (DM) variations which could cause significant uncertainties in the absolute timing of pulsars (Backer et al. 1993).

In the timing analysis, both sets of TOAs obtained at Effelsberg and WSRT were first independently fit to a pulsar spin-down model with the software package TEMPO¹. The resultant radio ephemerides were then used for aligning the RXTE data with the radio profiles, producing fully compatible results. Finally, we produced a best-fit timing model for PSR B1937+21, as given in Table 1, from the combined Effelsberg and WSRT TOAs to align the RXTE and radio data (see Fig. 1).

3. Pulse profile and phase analysis

RXTE data were searched for pulsed emission by using the folding technique in a range centered at a value computed from the ephemeris reported in Table 1. The plot of the χ^2 vs the pulsar frequency showed a clear single maximum, very prominent above the noise level and the pulsar frequency, estimated by fitting the χ^2 peak with

¹ <http://pulsar.princeton.edu/tempo>

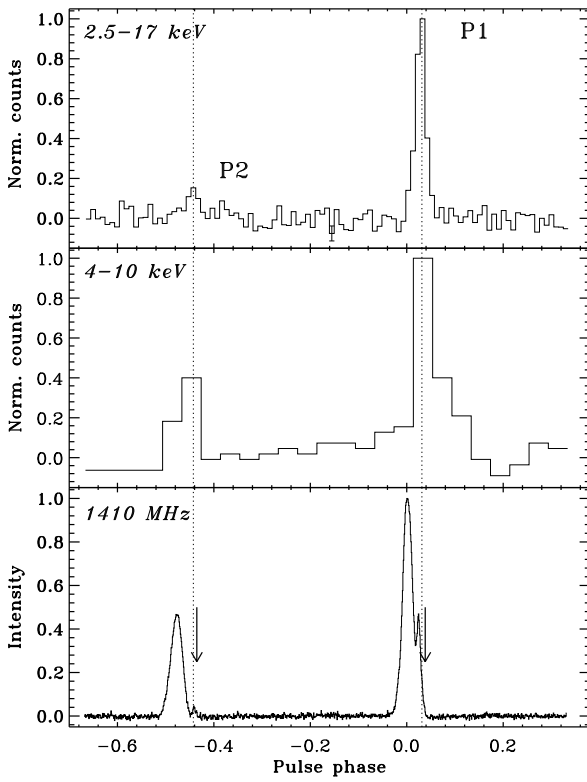


Fig. 1. **Top:** The RXTE pulse profile of PSR B1937+21 in the 2–17 keV energy band. The bin size corresponds to $\sim 16 \mu\text{s}$. **Middle:** The 4–10 keV BeppoSAX profile (Nicastro et al. 2002) with the P1 aligned with the P1 phase in the top panel. **Bottom:** Radio pulse profile at 1.6 GHz obtained from Effelsberg. Vertical arrows indicate the phases of observed radio giant pulses.

a gaussian profile, was $\nu = 641.92824453 \pm 2 \times 10^{-8}$ Hz in agreement within the errors with that from the radio timing model (Table 1).

The highest significance of the pulsation is reached in the energy interval 2.5–17.0 keV and the resulting X-ray pulse profile, obtained by folding the data with the radio frequency (Table 1), is shown in Fig. 1 (top panel). It is characterized by a prominent narrow first peak (P1), and by a less apparent second peak (P2). The significance of the latter is 5σ above the off-pulse level. P2 is lagging P1 by 0.526 ± 0.002 , determined by fitting both pulses with symmetric Lorentzian shapes. The detection of P2 is confirmed by the BeppoSAX data in which a second peak was detected at the same phase location (Nicastro et al. 2002). We show the BeppoSAX result in the middle panel of Fig. 1: this profile has been shifted to align P1 with the phase of P1 in the top panel. Pulse widths are wider in the BeppoSAX data likely because the events are affected by a less accurate time tagging. The P1 width (FWHM) measured in the RXTE profile is only $29 \pm 2 \mu\text{s}$ and the P2 width is $51 \pm 21 \mu\text{s}$. Fig. 1 (bottom panel) shows the radio profile from one Effelsberg observation. Vertical arrows

mark the phases of giant pulses (Kinkhabwala et al. 2000). The comparison in absolute phase between the X-ray and radio profiles shows that the P1 lags the main radio pulse by $44 \pm 1 \pm 8 \mu\text{s}$ and P2 lags the secondary radio peak by $51 \pm 3 \pm 8 \mu\text{s}$, where the quoted uncertainties are due to statistical error, source position inaccuracies and absolute timing precision of RXTE, respectively. The X-ray peaks appear closely aligned with the phase of the radio giant pulses. In addition, the phase separation between the X-ray pulses of 0.526 ± 0.002 is more consistent with the phase separation between the positions of the giant radio pulses (0.5264 ± 0.0006) than with that between the radio main and secondary pulses (0.52106 ± 0.00003). The latter makes a systematic difference in the absolute X-ray and radio timing as explanation for the shifts unlikely.

The occurrence of the same phases for the X-ray pulses and the radio giant ones suggests the possibility that high energy photons are emitted simultaneous with the latters. Therefore, we searched if there is some evidence for a bunching of X-ray photons with a rate similar to that of giant pulses and equal to ~ 4 pulses per minute (Cognard et al. 1996; Kinkhabwala et al. 2000). During the RXTE exposure we then expected that pulsed events occur in about 9000 X-ray flares. To investigate this hypothesis we made an X-ray light curve selecting only events within the phase interval centered in P1 with a phase width of $\Delta\phi = 0.06$ ($90 \mu\text{s}$) and studied the frequency distribution of these events. Since the dead time of the PCA is about $10 \mu\text{s}$ the maximum content of a bin in the presence of a X-ray flares cannot exceed 8–9 counts. We found the following statistics: 2 bins with 4 counts, 11 bins with 3 counts, 574 bins with 2 counts, 294 060 bins with 1 count and 92 208 884 with 0 count. This distribution is not consistent with the Poisson statistics, where the expected number of bins with a number equal or higher than 2 counts is much lower than measured. However, there is no evidence for the existence of X-ray giant pulses because the number of bins with a content different from the Poisson distribution was only 116, much lower than the number foreseen from the frequency of radio giant pulses. Another possibility is that the rate of X-ray giant pulses could be lower than that observed in the radio band and that the high energy emission could be a mix of steady pulsation plus some more rare giant pulse episodes. We constructed other light curves selecting events in 10 different phase intervals far from P1 and P2 and with the same phase width used in the selection of the P1 interval. We found similar deviations from the expected Poisson distribution in all light curves. In particular, the number of bins deviating from a Poisson distribution was found to be between 60 and 150. Therefore, we conclude that there is no evidence that the X-ray emission of PSR B1937+21 is bunched in relatively rare events of high intensity.

4. Spectral analysis

Pulse-phase histograms were evaluated separately for each unit of the PCA for the 256 PHA channels. Response

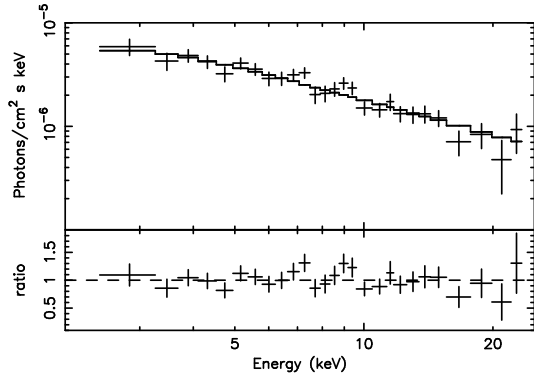


Fig. 2. The pulsed spectrum (P1) with superimposed the best fit power law model (**top**) and their ratio (**bottom**)

matrices and sensitive areas were then derived for each PCU and summed weighting them by the integrated background subtracted counts of the corresponding PCU's pulse phase histograms. Pulsed spectra of the main pulse were obtained accumulating in the phase interval 0.68–0.72 and subtracting the mean off-pulse level evaluated in the phase interval 0.27–0.65. Because of the low intensity of P2, its phase interval was not added to the pulsed signal. Spectra were finally combined by summing the individual PHA counts and assigned a total exposure time equal to the sum of the individual exposures. Furthermore, energy channels were rebinned to have a minimum content of 20 counts. The resulting pulsed spectrum in the range 2–25 keV was fitted with an absorbed power-law model with the interstellar hydrogen column density N_{H} fixed to $2.0 \times 10^{22} \text{ cm}^{-2}$ (Nicastro et al. 2003). The best fit pulsed spectrum gave a photon index of 1.14 ± 0.07 with a reduced χ^2 of 0.90 (47 d.o.f): it is shown in Fig. 2 (top panel) with the residuals in units of data to model ratio (bottom panel). These results are in agreement with those obtained from the analysis of the data of a BeppoSAX observation (Nicastro et al. 2003). The unabsorbed flux in the 2–25 keV band is $6.6 \times 10^{-13} \text{ erg cm}^{-2} \text{ s}^{-1}$ with the corresponding luminosity $L_X = 8.4 \times 10^{31} \Theta (d/3.6 \text{ kpc})^2 \text{ erg s}^{-1}$, where Θ is the pulsar beam size.

A fit with a black body model gives $kT = 2.6 \pm 0.1 \text{ keV}$, with a $\chi^2_r = 1.5$ (47 d.o.f). Although the fit is marginally acceptable, there are some systematic deviations in the residuals, and the derived temperature $T = 2.8 \times 10^7 \text{ K}$ is very high, particularly for an old recycled MSP.

5. Discussion

The RXTE observations of the millisecond pulsar PSR B1937+21 provided for the first time a detection of a pulsed emission up to an energy of 20 keV. Like in the radio, we find a double peaked pulse shape with a dominant first peak and a much weaker second peak. Despite being only weakly detected, its presence is confirmed by recent BeppoSAX data showing a second peak at the exact same location. The pulsed spectrum is remarkably hard with a photon index of 1.14 indicating that the X-ray emission

is non-thermal. The major finding of the present analysis is that the X-ray and radio pulses are not precisely aligned, but the formers lag the latters by a phase difference of 0.028 ± 0.006 (P1). The X-ray pulses are then very well aligned to the giant pulses observed in the radio band (Kinkhabwala & Thorsett 2000). Our result is not in agreement with the single peak profile at the same phase of the radio interpulse, reported by Takahashi et al. (2001) from ASCA data.

Phase coincidences between radio giant and X-ray pulses have earlier been reported by Romani & Johnston (2001) for the MSP PSR B1821–24. These authors predicted that PSR B1937+21 must also show the same property, which has now been confirmed. Among the ordinary pulsars, giant pulses are observed only from the Crab pulsar (e.g. Lundgren et al. 1995, Cordes et al. 2003) and very recently from PSR B0540–69 (Johnston & Romani 2003).

The fact that X-ray and giant radio pulses are observed in the same narrow phase intervals suggests that they are emitted from the same region of the magnetosphere. It is indeed very unlikely that travel time and aberration effects will combine themselves to give exactly the same phases. It is unknown if this region lies close to the polar caps or in some other region of the magnetosphere. According to the scenario proposed by Romani & Johnston (2001) these pulses are produced in the outer gaps where there is copious production of secondary e^+e^- pairs. In this respect it is important to note that PSR B1937+21 is the only known pulsar with an estimated magnetic field strength at the light cylinder larger than that of the Crab pulsar, while PSR B1821–24, has a field at the light cylinder similar to the Crab. Also PSR B0540–69 ranks near the top of the distribution of pulsars with strong B fields near the light cylinder (about half the strength of the Crab and PSR B1821–24). The X-ray pulsed emission should be characterized by a stable intensity, in fact we do not find evidence for any clustering in time that could indicate the presence of X-ray flares. An interesting possibility is that there are large instabilities affecting mainly the space distribution of secondary pairs rather than their number. Likely, the current across the gap should remain nearly constant. It is then possible that the amplitude of these spatial fluctuations may occasionally be very large to produce an enhanced coherence in the radio emission observed as giant pulses. We expect that these fluctuations occur over a very short distance scale, comparable or smaller than $c\Delta\phi/\nu \simeq 1.3 \times 10^5 \text{ cm}$, equal to a fraction of about 4.4×10^{-4} of the radius of the velocity-of-light cylinder, to keep the phase window of giant pulses of the order of $\Delta\pi = 2.8 \times 10^{-3}$, corresponding to 1° as found by Kinkhabwala & Thorsett (2000).

Acknowledgements. Radio results are based on observations with the 100-m telescope of the Max-Planck-Institut für Radioastronomie at Effelsberg.

References

Alpar, M. A., Cheng, A. F., Ruderman, M. A., & Shaham, J. 1982, *Nature*, 300, 728

Backer, D. C., Dexter, M.R., Zepka, A.Ng D., et al. 1997, *PASP*, 109, 61

Backer, D. C., Hama S., Hook S.V., 1993, *ApJ*, 404, 636

Backer, D. C.,& Sallmen, S. T. 1982, *Nat*, 300, 615

Becker, W., & Aschenbach, B. 2002, Proceedings of the Seminar on Neutron Stars, Pulsars and Supernova Remnants, Physikzentrum Bad Honnef, eds W. Becker, H. Lesch & J. Trümper

Bradt, H. V., Rothschild, R. E., & Swank, J. H. 1993, *A&A*, 97, 355

Cognard, L., Shrauner, J. A., Taylor, J. H., & Thorsett S. E. 1996, *ApJ*, 457, L81

Cordes, J. M., Lazio, T. J. W. 2002, *astro-ph/0207156*

Cordes, J. M., Bhat, N. D. R., Hankins, T. H., et al. 2003, *ApJ* submitted, *astro-ph/0304495*

Dickey, J. M., Lockman, F. J., 1990, *ARA&A*, 28, 215

Ho, C. 1989, *ApJ*, 342, 396

Jahoda, H. K. 1994, *AAS*, 26, 894

Johnston, S., & Romani, R. W. 2003, *ApJ*, accepted, *astro-ph/0305235*

Kinkhabwala, A., & Thorsett, S.E. 2000, *ApJ*, 535, 365

Lange, Ch., Camilo, F., Wex, N., et al. 2001, *MNRAS*, 326, 274

Lundgren, S. C., Cordes, J. M., Ulmer, M., et al. 1995, *ApJ*, 453, 433

Nicastro, L., Cusumano, G., Kuiper, L., et al. 2002, Proceedings of the Seminar on Neutron Stars, Pulsars and Supernova Remnants, Physikzentrum Bad Honnef, eds W. Becker, H. Lesch & J. Trümper

Nicastro, L., Cusumano, G., Mineo, T., et al. 2003, *A&A*, submitted

Romani, R. W. 1996, *ApJ*, 470, 469

Romani, R. W., & Johnston, S. 2001, *ApJ*, 557, L93

Sallmen, S., & Bacher, D.C. 1995, in *ASP Conf. Ser.* 72, Millisecond Pulsars: A decade of Surprise, ed. A. S. Fruchter, M. Tavani, & D.C. Backer (San Francisco: AOP), 340

Standish, E.M. 1982, *A&A*, 114, 297

Takahashi, M., Shibata, S., Torii, K., et al. 2001, *ApJ*, 554, 316

Taylor, J. H., & Cordes J. M. 1993, *ApJ*, 411, 674

Voûte, J. L. L., Kouwenhoven, M. L. A., van Haren, P. C., et al. 2002, *A&A*, 385, 733